Research Article

Geology, Spectrometric Prospecting and Rare Earth Elements Geochemistry of the Fluorite Mineralization at Some Localities Eastern Desert, Egypt

Gehad M. Saleh*, Mohamed Abd El Monsef, and Bahaa M. Emad

Abstract

The present work deals with the geology, radioactivity and geochemical investigations of rare earth elements associated with fluorite veins. The latter is intruded in granites with as a peculiar distribution of economically important mineralization and has a variety of colours (mostly green and violet) and occurs as banded with distinct alternation bands of silica and carbonate and also as veins. Field work spectroscopy measurements over these fluorite veins reveal that some veins are radiometrically anomalous. Geochemically, the averages of total rare earth elements (ΣREE) of fluorites are 178.44 ppm for G. Um Rekhta area, 135.28 ppm for G. Anwayib area, 184.17 ppm for G. Eir Arib area, 235.15 ppm for G. Homret Mikpid area and 179.79 ppm for G. Egat area. The LREE concentrations are dominantly higher than HREE concentrations and REE normalized patterns indicate decreasing abundances with increasing atomic number. All fluorites in the studied areas have strong positive Y anomalies are between 1.51 and 4.10 (with mean of 2.60), negative Eu anomalies are between 0.09 to 0.78 (with mean of 0.38) and slightly positive Ce anomalies are between 0.54 and 1.57 (with mean of 1.00). The Y/Ho values range from 36 to 118 with av. 77.18. The Tb/Ca and Tb/La ratios of the studied fluorites are intermediate to high and these ratios also indicate a formation of fluorites from fractionated ore-bearing fluids at an early stage of mineralization, mainly a hydrothermal stage. The hydrothermal fluids which formed the fluorites were probably derived from the granitic melt. Consequently, the field geology and REE geochemistry show that the composition of mineralizing fluids, the location of ore formations, the mineralizing mechanisms and the prevailing physicochemical conditions of the depositional environments for the fluorite veins of the studied areas were different. The high contents of radioactivity and rare earth elements mineralization in some fluorite veins make them a target to enlarge the potentiality of the highly mineralized localities

Introduction

Fluorite (CaF2), also commercially known as fluorspar, is an important mineral that is used as a raw material in the metallurgical, ceramic and chemical industries apart from optical and lapidary uses [1]. Fluorite occurs as an ore or a gangue mineral in all hydrothermal processes from the beginning of the pegmatitic phase to the end of the hydrothermal phase [2]. Therefore, investigation of the REE concentrations of fluorites occurring in different pegmatitic and hydrothermal stages has mostly been studied using geochemical exploration methods [3,4]. REE-rich ores in carbonatites and peralkaline igneous rocks can be directly derived from magmatic processes, but also from metasomatism and hydrothermal remobilization of magmatic REE minerals [5-11]. Fluorite may be deposited together with rare earth element (REE)- bearing minerals, in mining areas associated with pegmatitic and hydrothermal stages, in weathering and sedimentary environments within sedimentary, metamorphic and igneous rocks [12].

Fluorite is restricted to the younger granites of Eastern Desert of Egypt and some veins and pegmatites. It occurs as disseminations, as cavity and fracture filling. Sometimes it forms gangue mineral associated with rare-metal mineralization such as Sn and W that are closely related to GUI granite of [13] and are common as veins cutting the younger granites of Egypt [14-30]. The present work will shed the light on the formation conditions of fluorite and the concentrations of major, trace and rare earth elements (REE) geochemistry in fluorite from different localities in the Eastern Desert, Egypt

Geologic setting and petrography

Um Rakhat area

The studied area is covered mainly by Precambrian basement rocks including both syn-and post-tectonic granites overlain by nearly horizontal sedimentary strata of Nubian sandstones (Figures 1a-1f). El-Missikat pluton is an oval shaped, covering an area of about 75 km2, with its maximum length 12.5 km trending NW [31,20]. Three phases of El-Missikat monzogranite (MG) are recorded by [32,33] as shown in (Figure 1b). This granite is the most important rock containing the U-mineralized silica veins. The latter is affected by many alterations such as silicification, sericitization, thematicization (Figure 2a), kaolinization and dendritic manganese staining especially along fault and shear zones. The studied fluorite at Um Rakhat has a variable colour including blue, red, green and violet (Figure 2b) and is also found as massive bodies sometimes develop euhedral cubes on the surface. In many aspects, the granite becomes more radioactive than the around rocks due to the presence of fluorite zones with deep violet colours as a result of radioactivity (Figure 2c).

Homret Mikpid area

The investigated area is composed essentially of granitoid masses and metamudstones (Figure 1c). These granitoid masses are categorized as quartz-diorite, granodiorite and adamellite [34]. Several zones of beryl bearing pegmatite, quartz and fluorite veins occur in the northern part of the adamellite mass. At the north-eastern contact, two parallel beryl bearing pegmatite veins are observed within weakly greisenized and locally albitized granite. The fluorite veins are also recorded traversing the adamellite. The thickness of these veins ranges from 0.25 to 0.50 m and their length varies from 50 to 1000 m. Fluorite varies in color from light to deep green, pale yellow to pink and sometimes violet and are structurally controlled, trending NE-SW and NW-SE.

*Corresponding author: Gehad M. Saleh, Professor of Economic Geology, Head of Research Sector of Geology Nuclear, Materials Authority, Cairo, Egypt. E-mail: drgehad_m@yahoo.com
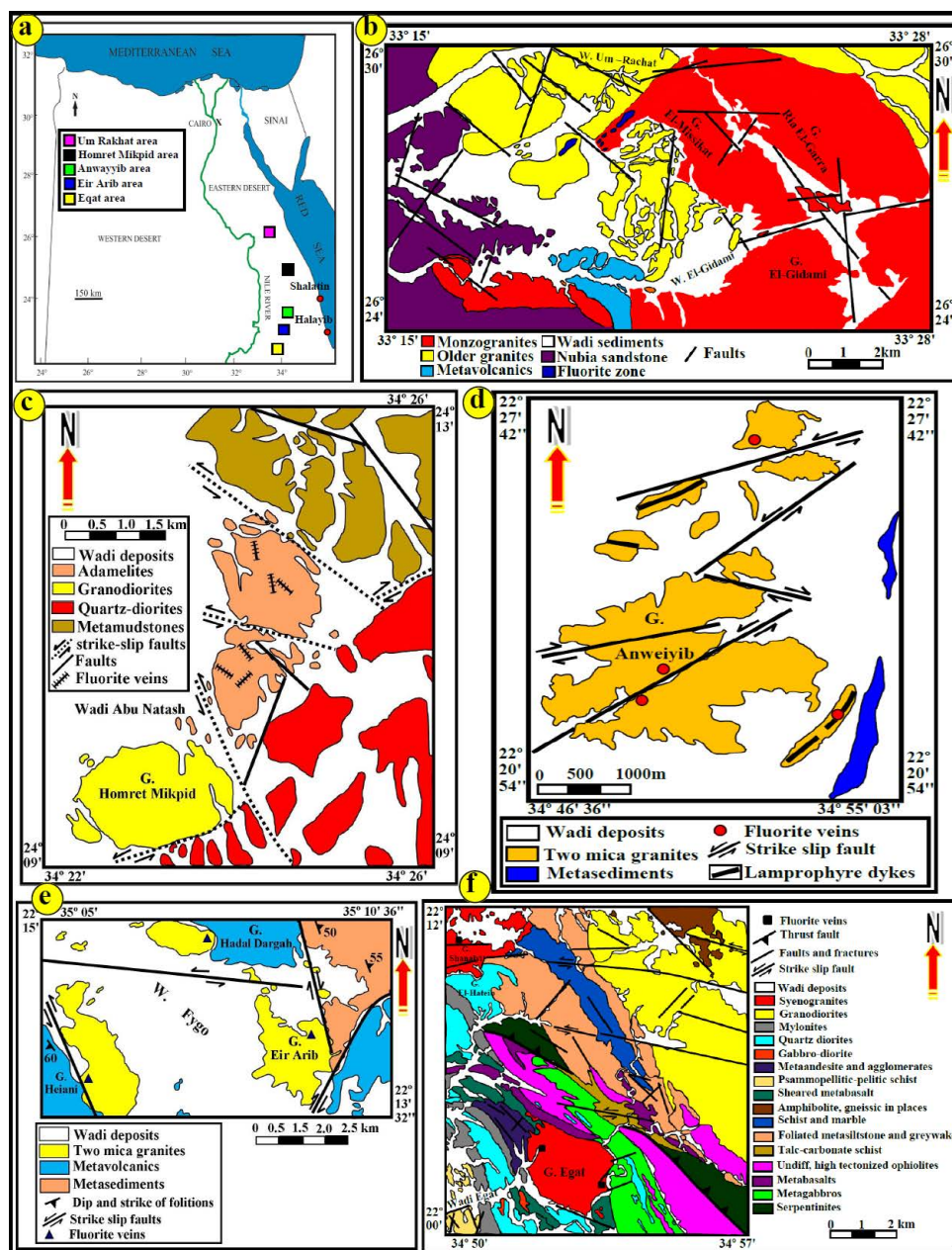
Figurw 1: a) Location map of the studied areas, b) A geologic map of El-Missikat-El-Aradiya area (Ibrahim), c) A geologic map of Homret Mikpid area (Saleh et al), d) A geologic map of the Anwayyib area (by G.M.Saleh), e) A geological map of Eir Arib area (Saleh and El Nisr,) and f) A geological map of G. Eqat area, SED, Egypt (Zoheir and Emam)
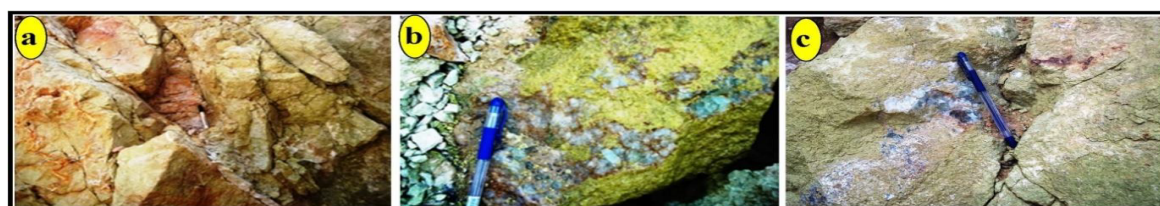
Figure 2: Field photographs of Um Rakhat area, CED, Egypt showing: a) Hematitization in illite zone with fluorite, b) Blue fluorite, and c) Deep violet and blue fluorite.

Anwayyib area

The studied area is situated in the extreme Southern part of the Eastern Desert Northwest Halayib (Figure 1d). It occurs as isolated pluton of two mica granites elongated in NW trend and covers an area of about 50 Km2. The major fluorite vein is about 50-100 m long and 0.25 to 0.50 m thick. Fluorite forms coarse-grained cubic crystals and grades in colour from honey to green while calcite is black and also occurs as intersected veinlets forming stock work up to 10 m width as well as disseminated crystals in the wall zone.

Eir Arib area

The studied area is composed mainly of peraluminous two-mica granites and lies along the Red Sea coast, about 130 km Southwest of Shalatin city (Figure 1e). It is dominantly covered by a Precambrian metamorphic sequence that is intruded by younger granitic intrusion. The metamorphic sequence including metavolcanics ortho-amphibolite and garnetiferous biotite schists [35]. The acidic dykes and fluorite veins are intruded in the two mica granites and highly affected by kaolinization and thematicization with the presence of carbonate and manganese oxides as thin films along fracture planes.

Egat area

The studied area is situated near the Egyptian-Sudanese border between latitude 22° 00′-22° 10′ N and longitude 34° 50′-35° 00′ E covering an area of 200 km2 (Figure 1f). It is composed mainly of ophiolitic ultramafic of serpentinites talc carbonate and talc graphite schist that occurs as elongated sheets and slices of NW-SE trend [36]. They thrust over sheared metavolcanics of meta-basalts and meta-andesite composition in association with meta-pyroclastic and metagabbro. Later, plutonic intrusions of gabbro-diorite, tonalite, and syeno granites forming G. Eqat mass intruded in the surrounding country rocks leaving marked of hydrothermal alterations. The main pluton of G. Eqat, which is composed mainly of cyanoguanides is dissected by many fluorite veins.

In hand specimen fluorite shows cubic habit and vitreous lustre and varies in colour white on the border of the vein changes gradually to green inwards and also pale to deep green colour (Figures 3a-3h). The zonal feature in colour of fluorite in different studied areas is possibly due to the formation from mineralizing solutions that had varied composition during deposition or due to its multiphase mode of formation [23]. Petrographically, Fluorite occurs as massive and coarse-grained crystals and are transparent, fractured and the fractures filled with fine grained quartz crystals and stained by radioactive minerals (Figures 4a-4c).

Materials and methods

The heavy minerals of fluorite samples were separated by using heavy liquid (bromoform) separation technique, followed by magnetic fractionation using Frantz isodynamic separator. The heavy minerals were picked under a binocular microscope and identified by Scanning Electron Microscope (SEM) at Nuclear Materials Authority (NMA) Laboratories, Cairo, Egypt. The major oxides were analysed by ICP-AES (Inductively coupled plasma atomic emission spectroscopy), F was analysed using a specific ion electrode, and trace elements and rare earth elements were analysed by ICP-MS; all analyses were performed by a commercial laboratory, Department of Earth Resources Engineering, Kyushu University, Japan, ACME Analytical Laboratories, Vancouver, Canada and Nuclear Materials Authority (NMA), Egypt (Table 1).

Results

Mineralogy and high-resolution textural analysis of the fluotite

The ESEM analysis of fluorite at G. Um Rakhat shows that, CaO (48.38 wt %) and F (19.45 wt %) (Figure 5a), the CaO (58.69 wt %) and F (35.75 wt %) at G. Homret Mikpid (Figure 5b), the CaO (74.66 wt %) and F (17.43 wt %) at G. Anwayyib (Figure 5c), the CaO (65.49 wt %) and F (34.51 wt %) at G. Eir Arib (Figure 5d) and the CaO (11.40 wt %) and F (16.88 wt %) at G. Eqat (Figures 5e and 5f).

Figure 3: Hand specimen photo of fluorite mineralization from studied areas, a, b and c) G. Um Rakhat, d) G. Homret Mikpid, e and f) G. Anwayyib, g) G. Eir Arib and h) G. Eqat areas, Eastern Desert, Egypt.
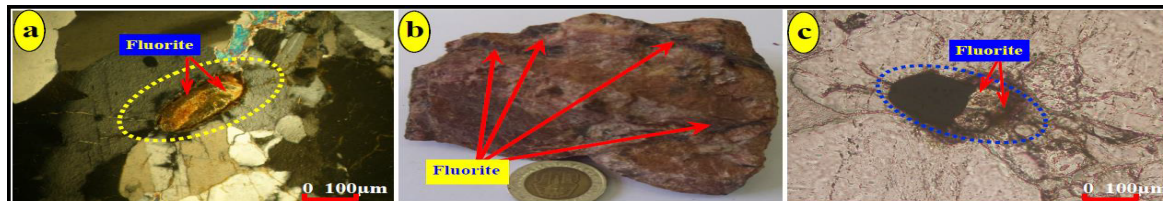
Figure 4: Photomicrographs of fluorite of studied areas, ED, Egypt, a) U-rich colloform banding fluorite (C.N.), b) Fluorite filling vugs in silica bands alternating with fluorite bands and c) Fluorite filling vugs with radioactive minerals (P.P.L.).

Table 1: Major oxides (Wt. %), Trace elements (ppm) and Rare earth element (REE) geochemistry of fluorite samples of studied areas, Eastern Desert, Egypt.

S. No.	3E	4E	5E	1HM	2HM	3HM	4HM	5HM	1EG	2EG	3EG	4EG	5EG
SiO_2	6.66	11.77	6.44	3.55	4.33	3.78	8.36	9.22	10.33	6.78	8.24	7.23	8.48
TiO_2	0.02	0.01	0.02	0.04	0.02	0.01	0.01	0.01	0.01	0.01	0.03	0.02	0.02
Al_2O_3	0.07	0.25	0.37	1.08	0.09	0.12	0.18	0.24	0.08	0.19	0.23	0.39	1.02
Fe_2O_3*	0.21	0.32	0.09	0.27	0.02	0.18	0.09	0.04	0.18	0.19	0.28	0.07	0.26
MnO	0.03	0.03	0.02	0.01	0.03	0.02	0.01	0.01	0.01	0.04	0.03	0.02	0.01
MgO	0.04	0.05	0.01	0.02	0.11	0.01	0.02	0.05	0.01	0.03	0.01	0.02	0.04
CaO	48.33	45.99	49.88	45.12	48.21	46.82	48.33	45.18	50.22	46.66	48.99	51.34	49.79
Na2O	0.03	0.02	0.07	0.05	0.02	0.05	0.03	0.06	0.02	0.02	0.03	0.07	0.04
K2O	0.27	0.17	0.24	0.16	0.03	0.14	0.09	0.06	0.04	0.32	0.17	0.28	0.22
P2O5	0.01	0.01	0.02	0.02	0.03	0.01	0.02	0.02	0.01	0.01	0.01	0.03	0.01
Cr2O3	0.133	0.012	0.048	0.188	0.026	0.045	0.012	0.122	0.199	0.136	0.078	0.096	0.178
Ca%	34.54	32.87	35.65	32.25	34.46	33.46	34.54	32.29	35.89	33.35	35.01	36.69	35.58
F%	40.0	38.0	40.0	44.0	45.0	47.0	41.0	42.0	38.0	42.0	39.0	39.0	37.0
U	3.9	12.3	6.5	4.2	3.1	2.8	2.7	3.1	12.6	5.6	10.7	8.2	4.2
Th	1.4	6.2	2.3	1.8	1.5	1.2	1.9	2.6	7.3	3.3	5.8	4.1	3.1
Y	342.0	409.0	260.0	720.0	845.0	754.0	732.0	833.0	789.0	693.0	645.0	542.0	633.0
Nb	4.0	5.6	9.8	3.7	6.4	7.9	6.3	4.2	7.5	3.4	4.2	5.6	8.7
Zr	6.0	8.0	4.0	14.0	4.6	11.3	9.6	8.8	7.6	6.4	9.4	5.4	10.2
Ni	2.0	2.0	4.0	4.0	5.0	3.0	2.0	5.0	7.0	6.0	5.0	3.0	2.0
Ba	104.0	158.0	175.0	66.0	20.0	25.0	30.0	10.0	24.0	60.0	35.0	45.0	55.0
Pb	89.2	102.3	64.2	39.7	55.5	45.3	24.8	78.5	65.9	77.4	55.8	44.1	88.6
Rb	3.8	2.4	1.9	2.7	1.5	1.2	4.2	0.7	0.6	2.2	3.3	3.8	1.4
Sr	56.0	88.0	63.0	81.0	74.0	66.0	85.0	69.0	75.0	82.0	71.0	75.0	88.0
Zn	189.0	369.0	520.0	423.0	126.0	321.0	115.0	49.0	89.0	145.0	178.0	245.0	298.0
As	8.6	14.6	17.9	1.1	0.9	0.7	0.5	0.6	0.6	0.7	0.4	0.3	0.8
Cu	4.1	7.8	9.5	7.8	10.6	12.6	34.2	10.6	9.5	11.4	5.4	3.8	7.1
Ag	0.2	0.6	0.3	0.1	0.4	0.1	0.40	0.2	0.2	0.4	0.1	0.1	0.5
Cs	3.2	2.2	5.8	7.3	9.5	3.6	5.8	6.6	7.9	10.4	4.5	6.5	7.9
Sc	2.0	3.0	3.0	1.0	3.0	4.0	2.0	2.0	2.0	3.0	3.0	5.0	2.0
Sn	8.0	4.0	1.0	6.0	3.0	2.0	5.0	7.0	3.0	4.0	3.0	2.0	5.0
Au	1.6	0.5	1.4	2.2	0.6	0.3	0.4	1.9	2.2	0.5	2.6	1.8	2.9
Mo	8.6	22.3	36.5	2.4	0.6	1.6	0.6	0.8	1.2	1.9	1.2	1.7	2.9
Hg	0.02	0.02	0.01	0.02	0.01	0.01	0.03	0.03	0.02	0.02	13.0	3.0	7.0
Co	2.0	4.0	5.0	7.0	10.0	5.0	14.0	22.0	2.0	4.0	0.4	0.6	0.9
Hf	1.2	1.4	2.7	0.6	0.8	0.7	0.6	0.3	0.3	0.5	14.9	11.6	13.7
Ga	10.4	14.3	13.2	14.8	12.5	14.6	12.3	11.4	8.0	10.2	0.03	0.01	0.04
Rare earth elements (ppm)													
La	14.5	22.4	10.3	24.5	24.3	16.8	12.4	11.7	18.3	20.1	16.7	11.2	8.9
Ce	20.1	35.3	60.2	75.9	48.9	37.7	26.9	28.1	37.4	39.7	25.8	28.6	16.8
Pr	3.80	5.20	8.30	14.50	5.24	4.61	3.88	4.22	4.45	5.21	4.33	3.91	2.88
Nd	16.6	11.6	40.5	45.8	22.9	18.7	16.5	19.3	20.4	22.7	17.5	18.7	13.7

Sm	10.50	21.60	8.60	50.30	9.52	8.45	10.25	11.45	8.69	9.66	8.67	9.78	6.59
Eu	0.90	2.45	1.80	5.90	0.56	0.36	0.69	0.98	0.74	0.66	0.59	0.45	0.85
Gd	16.50	25.80	14.80	30.20	22.99	17.33	22.34	25.46	22.12	18.56	19.78	15.66	14.88
Tb	4.70	10.20	4.80	15.30	7.63	5.89	8.45	6.65	8.96	6.35	7.66	6.45	4.88
Dy	50.70	22.90	14.90	30.80	44.98	36.45	39.22	45.22	42.32	33.62	37.61	30.23	29.33
Ho	3.30	8.90	7.20	9.70	9.77	7.88	7.56	10.23	8.66	8.76	6.55	7.58	8.22
Er	13.30	10.50	9.88	22.10	27.30	23.11	22.11	24.12	21.55	18.41	19.28	18.56	20.11
Yb	9.70	8.70	7.70	10.60	14.88	13.22	10.42	13.26	10.28	12.45	13.11	10.09	10.27
Lu	8.40	2.10	2.90	3.10	1.92	1.63	1.87	1.25	1.78	1.44	1.36	1.26	1.82
Tm	4.50	9.80	3.60	8.20	3.21	2.85	3.22	1.95	3.45	2.77	3.62	2.77	2.45
(La/Yb) n	1.01	1.74	0.90	1.56	1.10	0.86	0.80	0.59	1.20	1.09	0.86	0.75	0.58
(Tb/Yb) n	0.22	0.52	0.28	0.64	0.23	0.20	0.36	0.22	0.39	0.23	0.26	0.28	0.21
Eu/Eu*	0.21	0.32	0.49	0.46	0.12	0.09	0.14	0.18	0.16	0.15	0.14	0.11	0.26
Ce/Ce*	0.65	0.79	1.57	1.0	1.04	1.03	1.0	1.0	1.0	1.0	0.73	1.04	0.80
Y/ Y*	1.91	2.07	1.82	3.02	2.92	3.22	3.08	2.80	2.98	2.92	2.98	2.59	2.95
Y/Ho	103.64	45.96	36.11	74.23	86.49	95.69	96.83	81.43	91.11	79.11	98.47	71.50	77.01
La/Ho	4.39	2.52	1.43	2.53	2.49	2.13	1.64	1.14	2.11	2.30	2.55	1.48	1.08
Sc/Eu	2.22	1.22	1.67	0.17	5.36	11.11	2.90	2.04	2.70	4.55	5.08	11.11	3.53
∑LREEs	177.50	197.5	195.5	346.90	244.11	195.0	185.83	203.92	209.11	200.44	182.51	165.20	141.67

The obtained data from ESEM and back-scattered electron imaging (BSE) analysis of heavy minerals associated with the studied fluorite revealed the presence of uranothorite, columbite, galena, Zircon, pyrolusite and ilmenite (Figures 6a-6f).

Geochemistry of the fluorite mineralization

Representative chemical analyses of twenty-seven (27) of different colored fluorite from the different studied areas are listed in Table 1.

Major oxides geochemistry

Seven (7) fluorite samples of Um Rakhat area, five (5) fluorite samples of Anwayib area, five (5) fluorite samples of Eir Arib area, five (5) fluorite samples of Homret Mikpid area and five (5) fluorite samples of Egat area were analyzed for their major oxides, trace elements, and REE contents (Table 1). From this table we note that, the SiO_2, Al_2O_3 and Fe_2O_3 oxides have high contents in all the studied fluorite samples especially Fe_2O_3 oxide in Um Rakhat and Anwayibe samples which reflect the enrichment of uranium in these samples comparing with the others. But the other oxides (MgO, K_2O, Na_2O, TiO_2, P_2O_5 and MnO) have very low percent in all the studied fluorite samples.

Trace element geochemistry

All data of the trace elements were listed in Table 1, which shows that all the studied fluorite samples have high concentration of Y, Ba, Pb, and Zn but the highest values of Ba, Pb, and Zn were recorded in Eir Arib samples, the highest value of Y was recorded in Homret Mikpid samples and the highest values of uranium were obtained in Um Rakhat samples. On the other hand, the residual trace elements show normal or low concentrations in the studied fluorite samples, this means that all the studied fluorite samples derived associating to low differentiated magma and affect to low grade of alteration processes except Um Rakhat area which derived from high differentiated magma and high grade of alteration processes led to presence of uranium associations.

Rare earth element geochemistry

The REE concentrations in the studied fluorite samples are shown in Table 1. The mean ΣREE concentrations for the different fluorite samples range from 178.44 ppm for Um Rakhat area, 135.28 ppm for Anwayib area, 184.17 ppm for the samples of Eir Arib area, 235.15 ppm for the fluorite samples of Homret Mikpid area and 179.79 ppm for the fluorite samples of Egat area.

The chondrite-normalized REE patterns [37] of the fluorite samples of different studied areas manifested trends similar to each other and showed a decrease from high light REE (LREE) towards heavy REE (HREE) (Figure 7). In the studied fluorite samples, LREE concentrations are higher than HREE and therefore the alkali magmatic source is likely. Therefore, these results show that LREE enrichment in fluorites can denote an alkali magmatic source for the hydrothermal solution or metals and indicate early phases of fluorite mineralization [38-42]

Spectrometric Investigation

The instrument that used in the ground γ-ray spectrometric survey measurements is RS-230. Ground γ-ray spectrometric survey can detect dose rate (D.R.) in unit (nanosieverts per hour (nSvh−1)), potassium (K%), equivalent uranium content (eUppm), and equivalent thorium content (eTh ppm).Uranium mobilization (eUm) in the studied rock types can be calculated as follows: the uranium mobilization is calculated difference between the measured eU and the expected original uranium, which is calculated by dividing the measured eTh by the average eTh/eU ratio in the crustal acidic rocks (original uranium= eTh/3.5 according to Clark et al., [43-44]) to give the leaching values of uranium (eUm= eU-eTh/3.5). Positive values reveal uranium addition by mobilization, whilst negative values show migration of uranium by leaching.

Gamma Ray Spectroscopy and Radiometric Investigations

The results of spectrometric data were cured statistically (Table 2) to define the distribution characteristics of radioelements and their ratios in the granites and associated fluorites for different studied areas. The field spectrometric measurements detected localization of spectrometric anomaly associated with the fluorite veins of different studied areas. The statistical treatment of radiometric data is revealed on binary diagrams of eTh against eU, eU against eU/eTh and eU against eU-eTh/3.5. From these results, the host rock of the studied areas shows low enrichment by U-mineralization, whilst the fluorite veins reveal high concentrations of uranium.
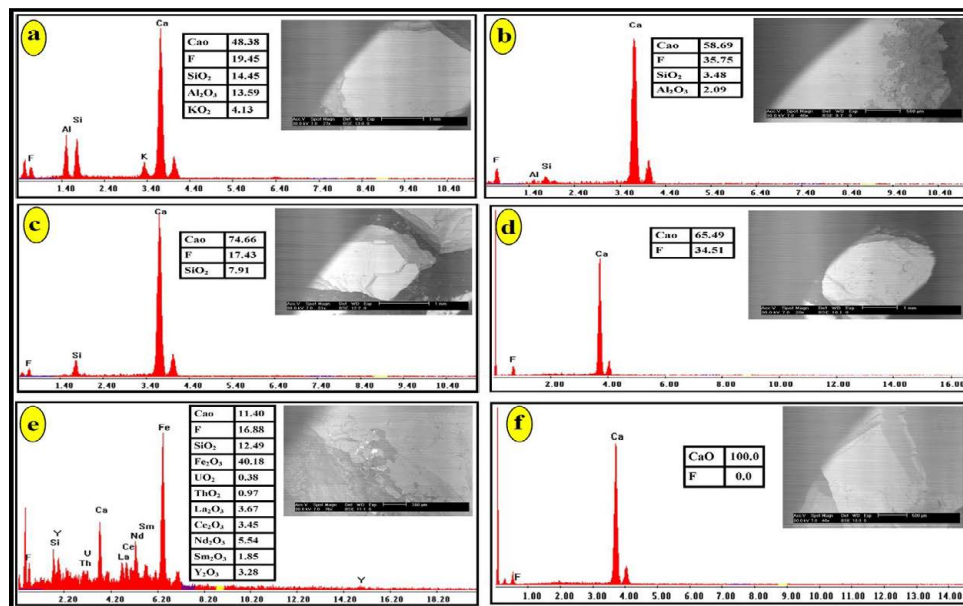
Figure 5: SEM image and EDX analysis data of fluorite mineralization for the a) G. Um Rakhat, b) G. Homret Mikpid, c) G. Anwayyib, d) G. Eir Arib and (e and f) G. Eqat areas, Eastern Desert, Egypt.
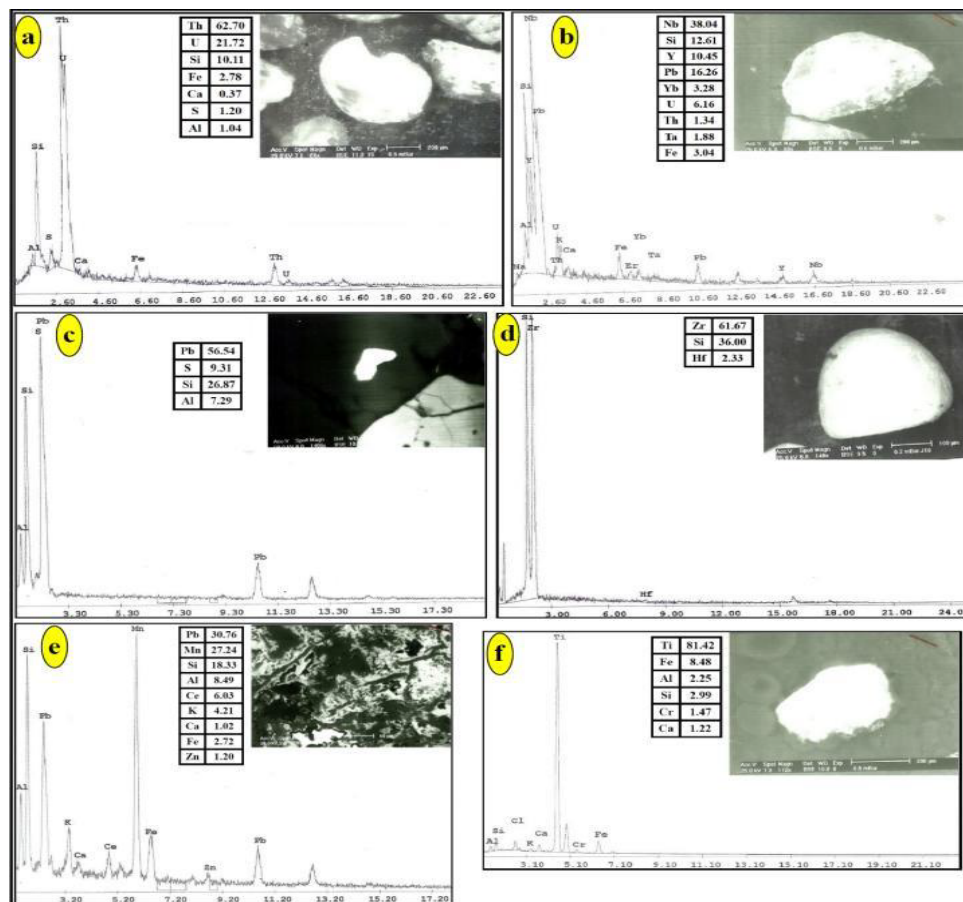

Figure 6: EDX and BSE image showing a) uranothorite, b) columbite, c) galena, d) zircon, e) pyrolusite and f) ilmenite minerals, studied areas, Eastern Desert, Egypt.
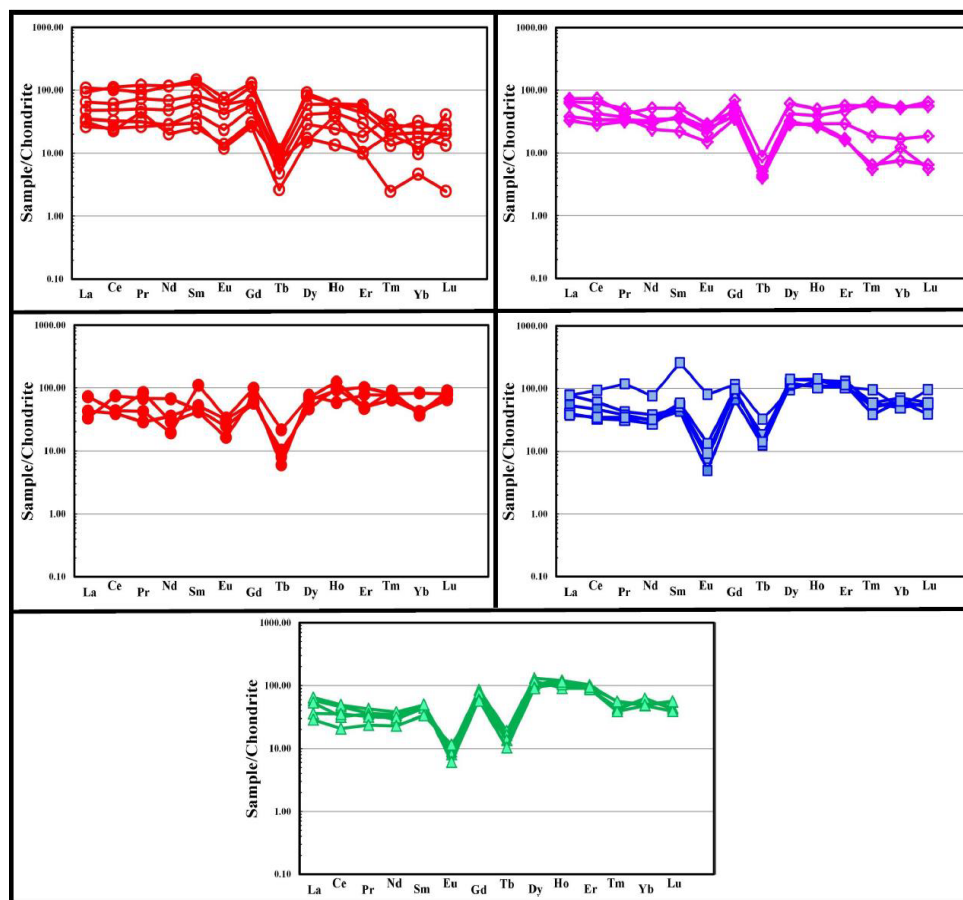
Figure 7: Chondrite-normalized REE patterns presented separately for all fluorite samples in areas, ED, Egypt (Boynton, 1984). Symbols are the same for all next diagrams (El-Missikat (Um Rakhat) area, Anwayib area, Er Arib area, G. Homret Mikpid area and G. Egat area), Eastern Desert, Egypt.

Table 2: Summary of the statistics for the three radioelements K, eU, eTh and their ratios for granites and fluorites of studied areas, Eastern Desert, Egypt.

	D.R. (mSv/y)	K%	eU(ppm)	eTh(ppm)	eU/eTh	eTh/eU	eU-(eTh/3.5)
Younger Granites (El-Missikat - Um Rakhat) area							
Minimum		2.50	7.20	17.80	0.16	1.64	-5.40
Maximum		11.30	16.70	66.60	0.61	6.13	6.41
Mean(X)		4.67	11.11	36.42	0.33	3.29	0.71
No. of Reading	49						
Fluorites (El-Missikat - Um Rakhat) area							
Minimum		3.90	20.00	42.00	0.33	0.84	2.46
Maximum		12.20	67.10	66.40	1.19	3.07	49.61
Mean(X)		7.24	49.08	52.16	0.94	1.14	34.18
No. of Reading	39						
Younger Granites (Anwayib area)							
Minimum	54.50	0.70	2.20	2.00	0.16	0.37	-2.89
Maximum	662.10	8.30	25.50	51.30	2.70	6.16	13.01
Mean(X)	142.96	3.33	6.50	13.71	0.58	2.14	2.59
No. of Reading	99						
Fluorites (Anwayib area)							
Minimum	54.30	0.70	0.40	0.10	0.05	0.11	-7.64
Maximum	737.80	8.50	54.80	98.50	9.00	21.33	26.66
Mean(X)	179.90	3.93	8.01	19.92	0.86	2.52	2.32
No. of Reading	50						
Younger Granites (Eir Arib area)							

|							
Minimum	12.50	0.20	0.30	0.20	0.14	0.14	-2.36
Maximum	537.10	7.40	36.50	55.80	7.00	7.33	20.56
Mean(X)	182.93	3.60	8.02	21.67	0.45	2.84	1.83
No. of Reading	150						
Fluorites (Eir Arib area)							
Minimum	28.00	0.60	0.50	2.80	0.14	1.1	-6.10
Maximum	673.50	6.10	48.60	90.70	0.90	7.0	22.69
Mean(X)	205.68	3.42	9.73	26.89	0.38	3.02	2.04
No. of Reading	50						
Younger Granites (G. Homret Mikpid area)							
Minimum	58.20	1.10	2.20	4.70	0.10	1.3	-6.77
Maximum	689.60	9.60	51.00	93.30	0.72	10.47	29.94
Mean(X)	341.96	5.42	16.44	45.46	0.36	3.04	3.45
No. of Reading	150						
Fluorites (G. Homret Mikpid area)							
Minimum	6.00	0.10	0.40	0.30	0.10	0.3	-102.90
Maximum	2724.90	6.80	145.20	635.30	3.33	10.36	74.73
Mean(X)	555.77	3.24	29.39	95.50	0.37	3.24	2.11
No. of Reading	239						
Younger Granites (G. Egat area)							
Minimum	57.30	1.00	1.30	6.60	0.17	1.09	-2.53
Maximum	221.10	4.20	11.00	36.20	0.92	6.0	7.43
Mean(X)	132.05	3.24	5.26	14.17	0.40	2.80	1.21
No. of Reading	200						
Fluorites (G. Egat area)							
Minimum	58.30	0.90	2.10	5.80	0.16	1.5	-12.66
Maximum	561.00	4.60	36.60	103.80	0.66	6.11	13.40
Mean(X)	167.04	2.26	8.11	23.94	0.36	3.01	1.27
No. of Reading	103						

Discussion

Trace element ratios

The Y and Y/Y* ratios in the studied fluorites samples had increasing values indicating an increase from the early mineralization stage to the late mineralization stage [45]. The Y/Ho ratio of the studied fluorites samples ranges between 36.11 and 118.06 with a mean of 77.18 (Table 1). The increasing Y/Ho ratio and positive Y (Y/Y*) anomalies of fluorites indicate interaction with a fluorine-rich aqueous fluid [46]. As a consequence, the Y/Ho ratio and positive Y anomaly may increase in the fluorites of different studied areas during the interaction of a fluorine-rich aqueous fluid in fluorine-rich milieus with host rocks. The fluorite samples of different studied areas display a wide range of La/Ho values, as revealed in (Figure 8a), but a narrow range of Y/Ho values. This could reflect either the partial loss of a LREE enriched phase or the formation of an enriched LREE phase during fluorite recrystallization [46]

The Y and Ho have a similar ionic radius and potential, and the Y/Ho ratios of the fluorite can be used to reveal the source of the fluid [46]. The Y/Ho ratios of the fluids with the same source are consistent and the Y-Ho fractionation will result in a significant change in the Y/Ho ratios [47]. The Y/Ho ratios of the studied fluorite samples are low, indicating the addition of exogenous fluid (Figure 8a). Also, the ratios of Y/Ho are relatively consistent in all the studied fluorite samples (46.1-58.9, 47.5-89.2, 33.3-48.8, respectively). Therefore, the same stage fluorite has a similar degree of Y-Ho fractionation and an identical fluid source. As shown in (Figure 8a) the Y/Ho ratios for the quartz and fluorite are within a narrow range of 35-100. Meanwhile, the La/Ho ratio for early-stage fluorite is slightly

higher than that of late-stage fluorite, suggesting that these minerals share a common origin and that recrystallization may occur in late hydrothermal stages [46]. In this study, the Y content in fluorite samples has a positive correlation with ΣREE (Figure 8b), therefore, Y preferentially remains in F-rich fluids. The late-stage fluorite crystalized from the fluids with increasing Y contents and Y/Y* ratios fractionation of the hydrothermal fluids because lanthanum and terbium are fractionated strongly by fluorite. These ratios have therefore been used to differentiate the physio-chemical conditions and environment of fluorite formations [38]. These ratios can be used to classify fluorites according to their different formation conditions such as hydrothermal, sedimentary and pegmatitic [48]. The high Tb/Ca ratios and the low Tb/La ratios also revealed fluorite formation from fractionated ore-bearing fluids at an early stage of mineralization [49]. All values for fluorite samples of different studied areas fall into hydrothermal field (Figure 8c). The (Tb/Yb) n-(La/Yb) n ratios show the order of crystallization as proposed by [39]. In fluorite samples of different studied area (Figure 8d), these two ratios are low because these fluorites are not LREE rich when compared to other fluorite deposits such as those in New Mexico, the Chloride District and Akdagmadeni [50,39]. The (La/Yb) n-(Eu/Eu*) n plots of the fluorite samples of different studied areas also show negative Eu anomalies and low LREE enrichments (Figure 8e).

The Sc/Eu vs Sr diagram (Figure 9a) reveal that, the studied fluorite samples fall into two distinct areas as the Rift deposits of New Mexico [39] and the fluorite deposits of Buyukcal and Akcakisla and shows that the studied fluorite samples have low Sr contents and high Sc/Eu values. Similarly, the Sr-(Eu/Eu*) n diagram reveals that both Sr and (Eu/Eu*) n values are very low and all samples have negative
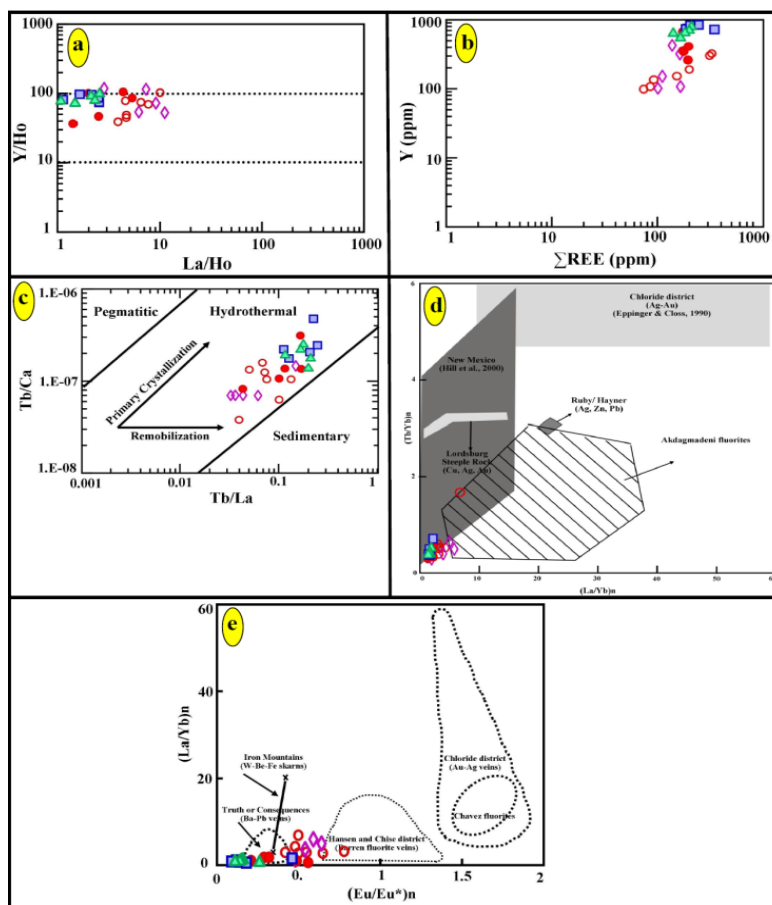
Figure 8: a) Y/Ho versus La/Ho ratios (Irber et al.,), b) Y versus ∑REE, c) Tb/Ca versus Tb/La variation diagram (Möller et al., Möller and Morteani,), d) (Tb/Yb) n ratio versus (La/Yb)n ratio (Eppinger and Closs, Hill et al, Sasmaz et al) and e) Chondrite normalization for the (La/Yb)n versus (Eu/Eu*)n diagram (Sasmaz et al, Uras and Çaliskan), for the studied fluorites samples, ED, Egypt

Eu anomalies (Figure 9b). The Sc values of the studied fluorite samples (Figure 9c) were similar to the fluorites of the Buyukcal and Akcakisla of New Mexico [40]. Overall, the trace element contents of the studied fluorite samples, ED, Egypt vary only weakly within the same deposit. The elements (W, Sn, and Mo) in stage fluorite from the studied areas are significantly higher (Figures 9d and 9e). Compared to the average value of the upper crust (Clark value) in stage fluorite, the enrichment coefficient of W, Sn, and Mo is 2.94, 0.98 and 0.37 in fluorite from the areas.

Eu, Ce and Y anomaly

Eu anomaly (Eu/Eu*=Eun/√ [Smn *Gdn]) and Ce anomaly (Ce/Ce*= Cen/√[Lan *Prn]) can be useful indicators for the features of fluids, such as temperature, pH and FO2 [51,52]. The studied fluorite samples have slightly positive Ce anomalies, between 0.54 and 1.57, with a mean of 1.00 (Table 1). Constantopoulos [49] proposed that, positive Ce anomaly in fluorites depends on high oxygen fugacity in the source of the hydrothermal fluids because of the resultant oxidation of Ce3+ and immobilization of Ce4+.

Fluorite samples in the different studied areas have negative Eu anomalies, demonstrated by a value lower than 1, with a range of 0.09 to 0.78 (mean: 0.38) (Table 1). These negative Eu anomalies elucidate the existence of Eu2+ during deposition of fluorites and low oxygen fugacity conditions of the hydrothermal solutions. The

fluorite precipitated from fluids with increasing FO2 or decreasing temperature or alternatively co-precipitated together with Eu-enriched minerals. All these reasons can expound how the negative Eu anomalies of the studied fluorite samples can be related to one or a few factors, such as a decrease in temperature or increases in FO2 and pH [6, 45]. Schwinn and Markl [53] also proposed that, the reduction of Eu3+ to Eu2+ happens at high temperatures and those hydrothermal fluorites above 200 °C show Eu-enrichment relative to the fluids.

Fluorite samples in the different studied areas reveal strong positive Y anomalies (Y/Y*=Yn/√ (Dyn *Hon) between 1.51 and 4.10 with a mean of 2.60 (Table 1). Möller and Holzbercher [54] proposed that, Y enrichments depend on the presence of fluoride complexes, while Bau [55] mention that, Y-F complexes have high stability when compared with Ho-F complexes. Therefore, Y outshines to stay within fluorite formed from F-rich fluids. Positive Y anomalies articulate strong complexation with F and decoupling of Y from HREE is a common feature in hydrothermal fluids dominated by F complexes [56].

Uranium and Thorium Radioactivity

The eU/eTh ratios reveal that the studied fluorite samples have a very high U potential mobilization and their ratios are not normal and
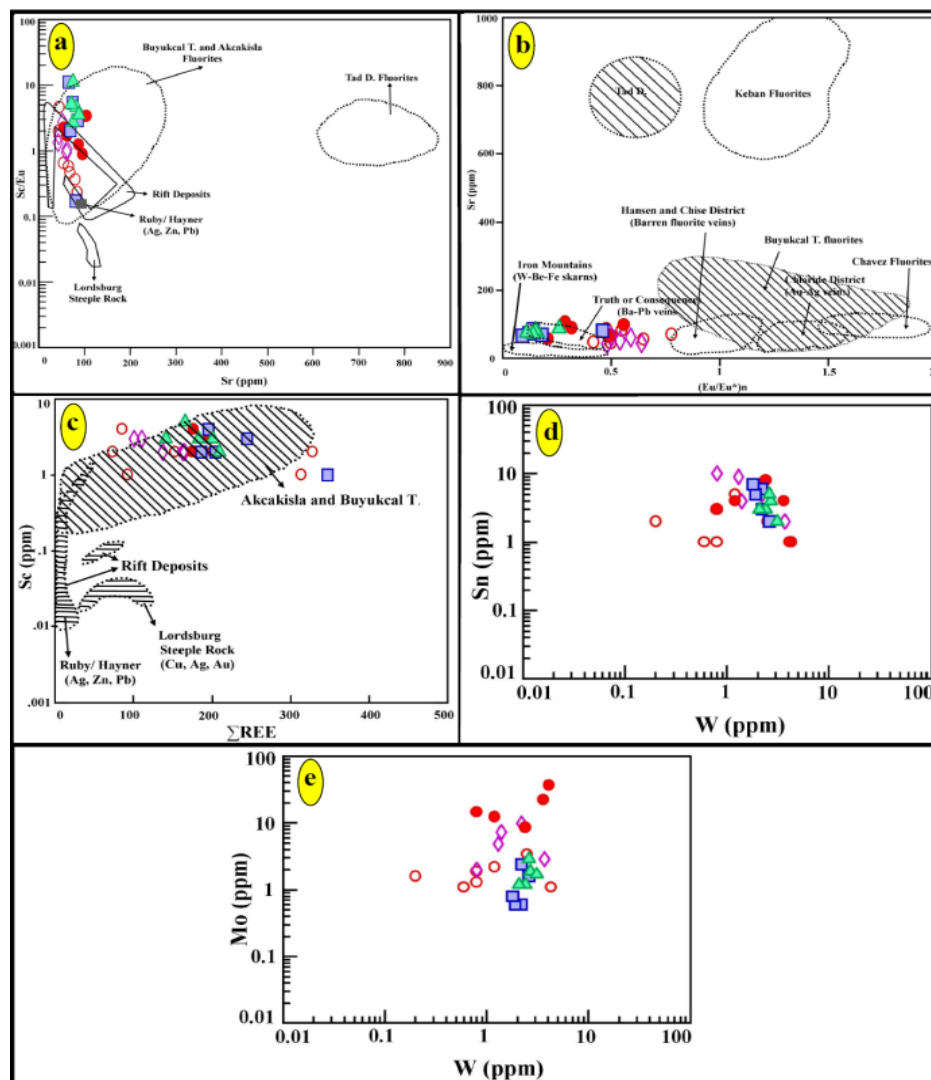
Figure 9: a) Sc/Eu ratios versus Sr ppm diagram, b) Sr versus (Eu/Eu*) n diagram, c) Sc versus ΣREE diagram (Sasmaz et al,), d) W versus Sn and e) W versus Mo for for the studied fluorites, ED, Egypt.

form anomalous zones. The eTh-eU diagrams in granites of different studied areas and their associated fluorites (Figures 10-14 a, d) reveal an enrichment of uranium where the highest eU and eTh contents are for the fluorite samples. Most of the studied fluorite samples have eTh/eU ratio between 0.11 and 21.33 with a simultaneous increase in both eU and eTh. Uranium remained relatively immobile in the original rock. According to this model, the radioelement increases gradually during magmatic fractionation, but the ratio changes due to different alteration processes [57]. Most of the studied granite and fluorite samples have higher uranium content (Table 2) than that of the hypothetical uranium distribution (Figures. 10-14 c, f) and so the mobilization gives positive values, which in turn indicates that U of these samples is leaching in [58]. The high uranium levels in fluorite samples of different studied areas (Table 2) may propose that the parent fluids were strongly oxidized, as uranium is very mobile under oxidizing conditions. On the other hand, it is possible that the parent fluids interacted with granites of different studied areas (host rock), which may be the source of uranium in reduced or weakly oxidized zones. This may find support by the slightly Ce positive anomalies in the associated fluorites.

Conclusions

Um Rakhat, Homret Mikpid, Anwayyib, Eir Arib and Egat rare metal bearing granites are dissected by a number of fluorite veins. These veins are trending NE-SW and NW-SE in conformity with the general trend of faults crosscutting the host rock. Geochemically, the studied fluorites are enriched in Ba, Zn, Y, Pb, Sr REEs and depleted in Rb, Zr and Nb contents. The chondrite normalized patterns of the studied fluorite veins reveal relative enrichment in the LREEs compared with the HREEs, this indicates that REE leaching from source rocks and fluid migration occurred under high-temperature and low-pH conditions. However, Tb/Ca–Tb/La ratios reveal distinct differences in the nature of the mineralizing fluids. The intermediate to high ratios of the studied fluorites are products of late-stage differentiate from hydrothermal fluids. The geological and geochemical data from the fluorites support the conclusion the fluorites of different studied areas were deposited from F-bearing hydrothermal fluids circulating within the granitic rocks.
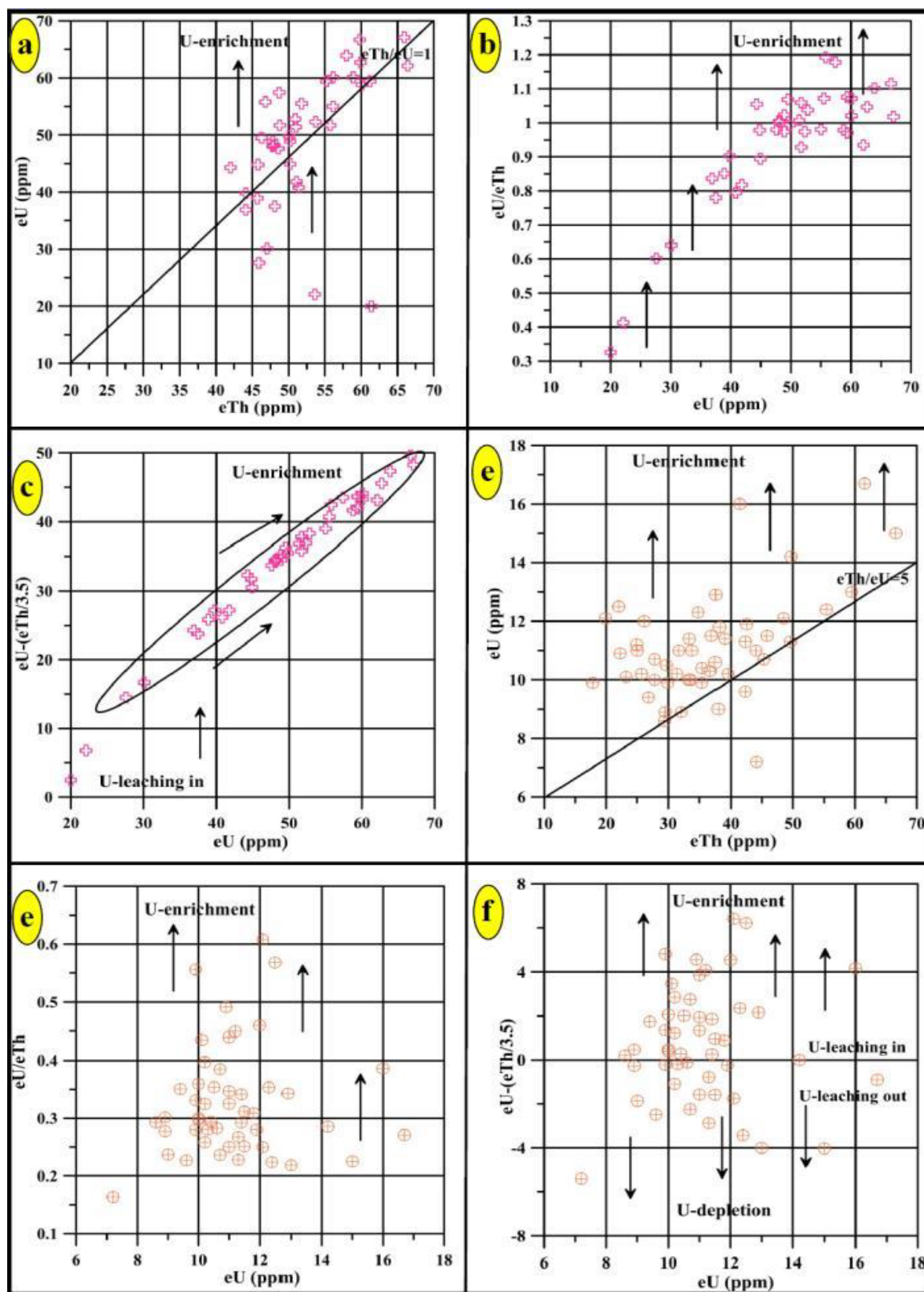
Figure 10: Radioactive elements plots of fluorite (from a to c) and granites (from d to f) at Um Rakhat area, Eastern Desert, Egypt
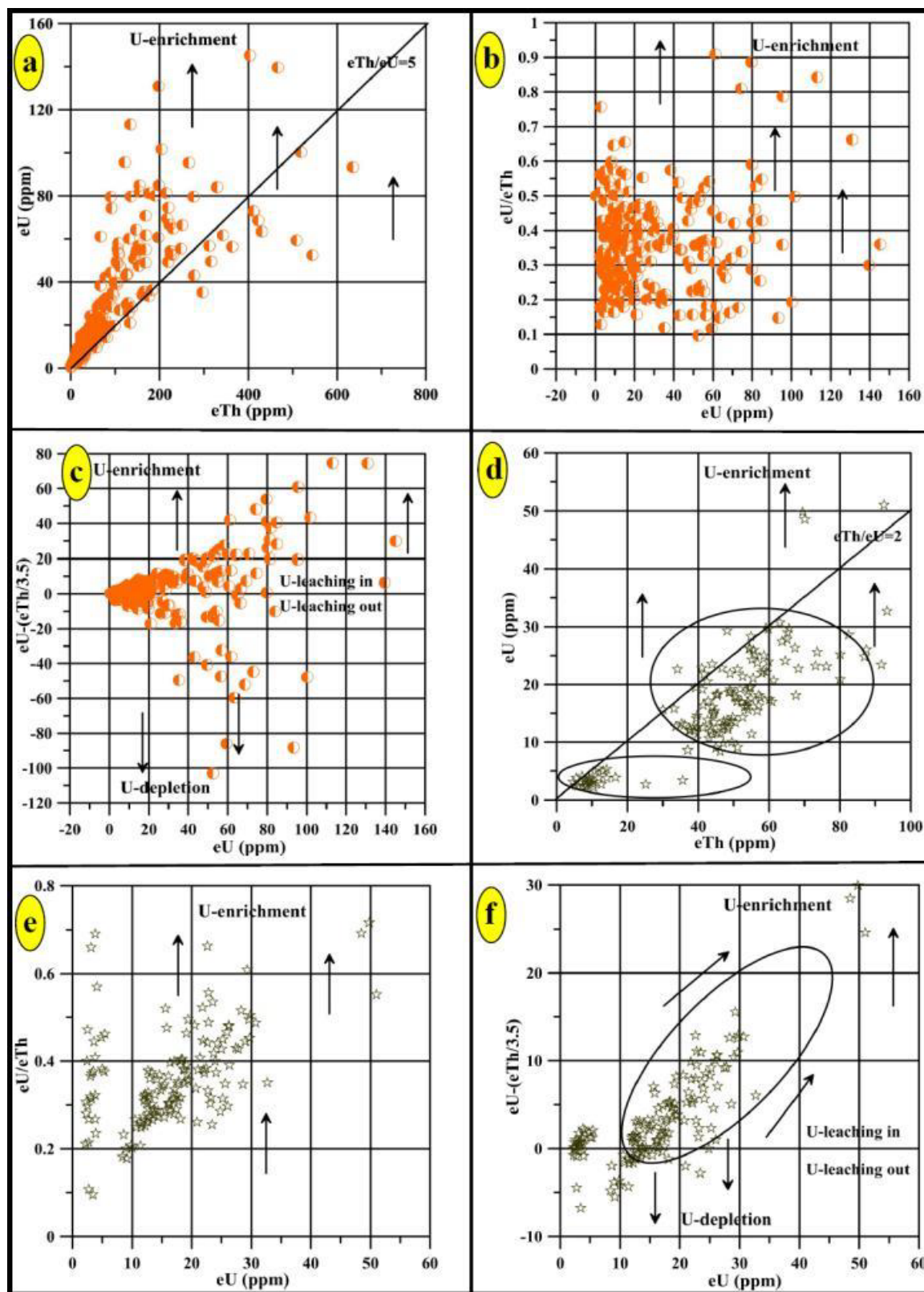
Figure 11: Radioactive elements plots of fluorite (from a to c) and granites (from d to f) at G. Homret Mikpid area, Eastern Desert, Egypt.
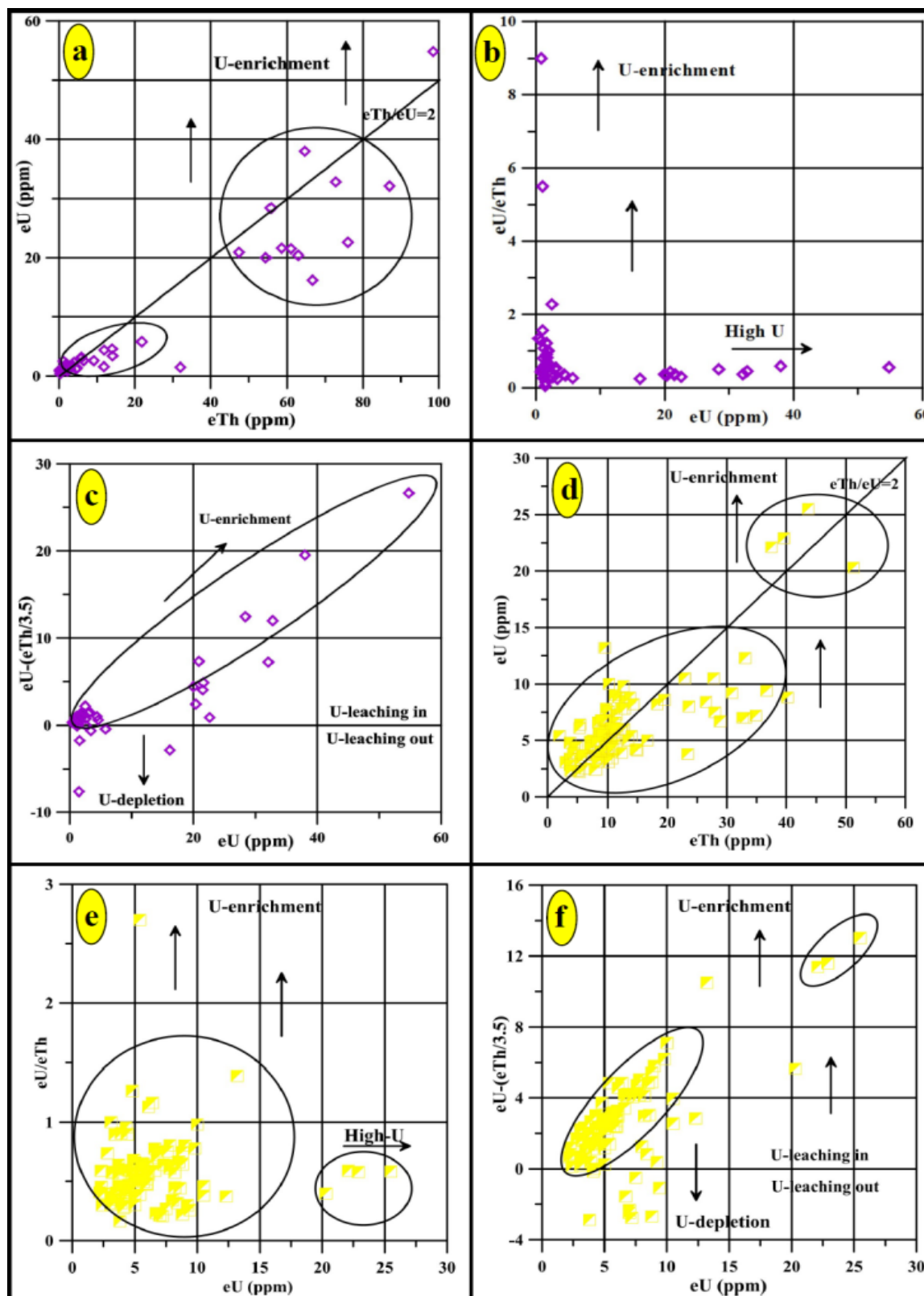
Figure 12: Radioactive elements plots of fluorite (from a to c) and granites (from d to f) at Anwayib area, Eastern Desert, Egypt.
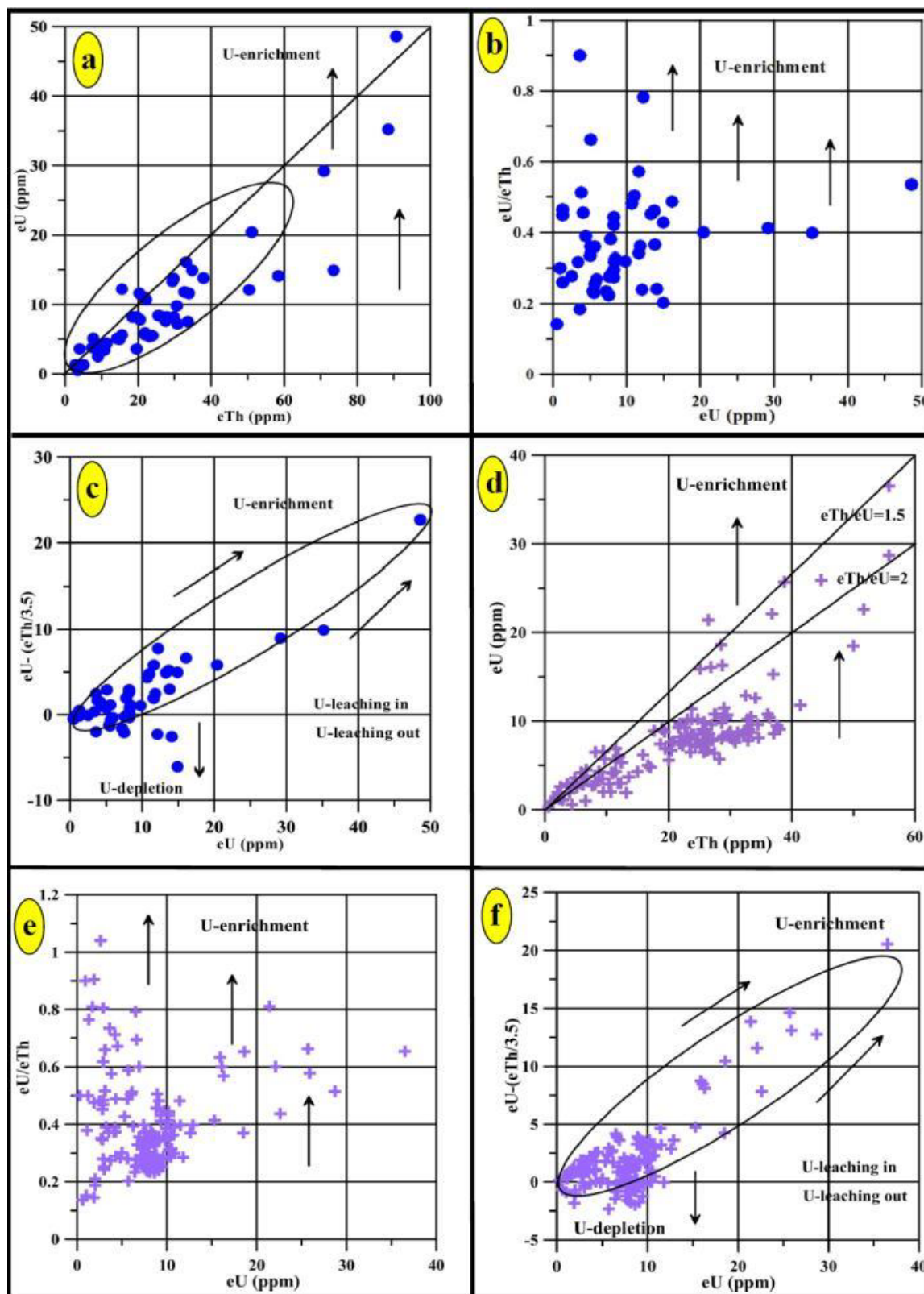
Figure 13: Radioactive elements plots of fluorite (from a to c) and granites (from d to f) at Eir Arib area, Eastern Desert, Egypt.
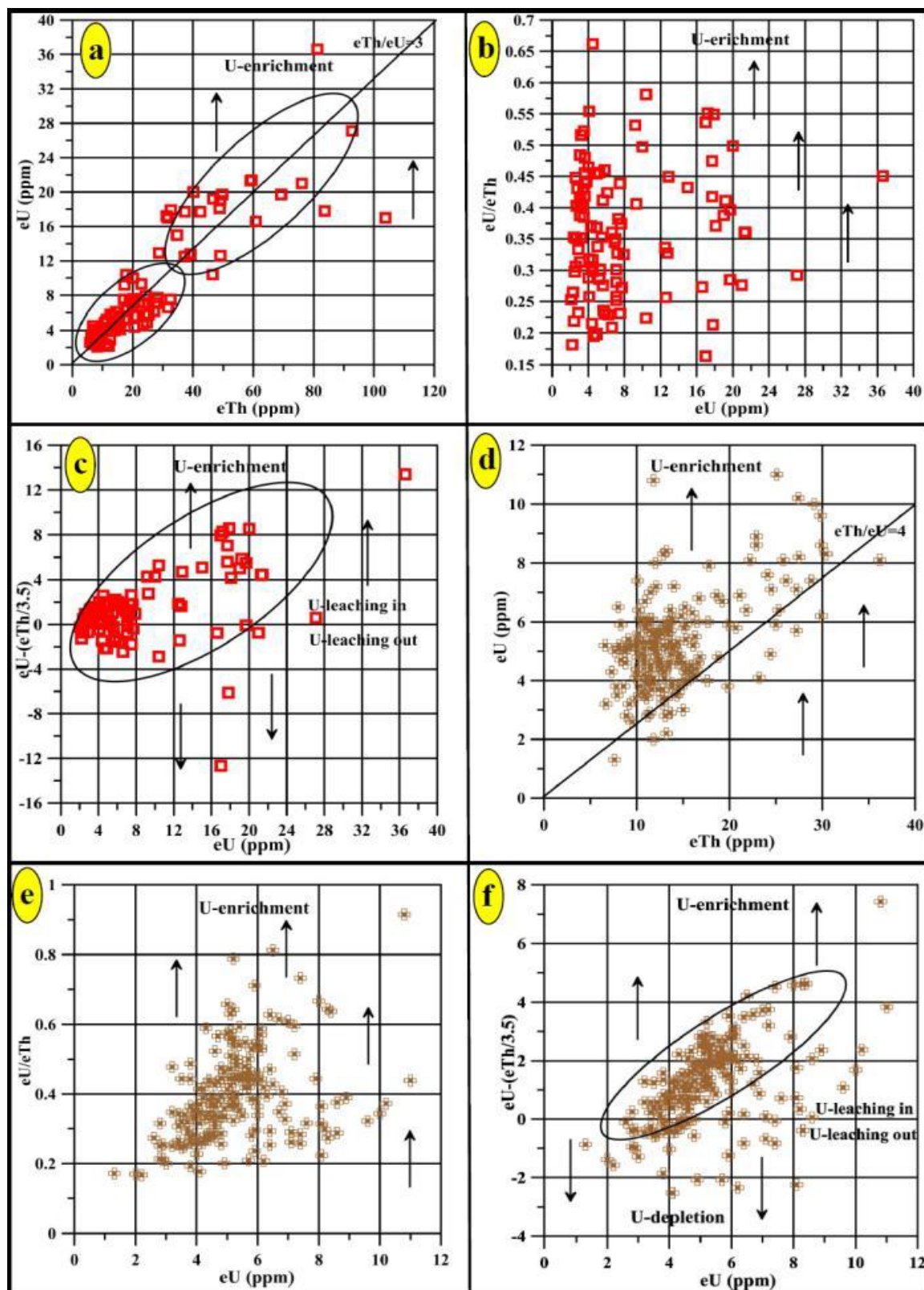
Figure 14: Radioactive elements plots of fluorite (from a to c) and granites (from d to f) at G. Egat area, Eastern Desert, Egypt.

All Fluorites in the studied areas display relatively high rare earth and Y (REY) contents, strong positive Y anomalies are between 1.51 and 4.10 (with mean of 2.60), negative Eu anomalies are between 0.09 to 0.78 (with mean of 0.38) and slightly positive Ce anomalies are between 0.54 and 1.57 (with mean of 1.00). These features indicate that the REY were mobilized mainly from non-carbonate rocks. The fluorite is associated and concurrent with the uranium mineralization, supplying evidence that the origin of uranium transported as uranium–fluoride complexes. The fluorine is the main factor for mobilization and enrichment of uranium in the late stage magmatic residual fluids through fractional crystallization and then hydrothermal solutions.

In our opinion, the exploration of REE-minerals in the fluorite veins may open interesting perspectives for the discovery of economic REE contents in this type of deposits, where REE could be recovered as by-product of the fluorite utilization. Furthermore, REE minerals could possibly be present also in dumps and tailings accumulated during the fluorite concentration process.

Acknowledgments

References

1. Magotra R, Namga S, Singh P, Srivastava P (2017) A New Classification Scheme of Fluorite Deposits. International Journal of Geosciences.8:599-610.

2. Pohl WL (2011) Economic Geology: Principles and Practice.Willey Blackwell, Oxford.663.

3. Souissi F, Radhia S, DandurandJ (2010) The Mississippi Valley-Type Fluorite Ore at Jebel Stah (Zaghouan District, North-Eastern Tunisia), Contribution of REE and Sr Isotope Geochemistries to the Genetic Model. Ore Geology Reviews.37:15-30.

4. Uras Y, Caliskan V (2014) Geochemical Patterns of the Buyukkizilcik (Kahramanmaras) Fluorite Deposits. Geochemistry International.52:1087-1100.

5. Samson I, Wood S, Finucane K (2004) Fluid inclusion characteristics and genesis of the fluorite– parisite mineralization in the snowbird deposit, Montana.Econ. Geol.99:1727-1744.

6. Farhad E (2012) Variation of mineralizing fluids and fractionation of REE during the emplacement of the vein-type fluorite deposit at Bozijan, Markazi Province, Iran.Journal of Geochemical Exploration.112:93-106.

7. Alexander P, Williams E (2013) Hydrothermal mobilization of pegmatite-hosted REE and Zr at Strange Lake, Canada: A reaction path model. Geochimica et Cosmochimica Acta.122:324-352

8. Akgul B (2015) Geochemical associations between fluorite mineralization and A-type shoshonitic magmatism in the Keban-Elazig area, East Anatolia, Turkey.J.Afr.Earth.Sci.111: 222-230

9. Alipour S, Ali A, Babak T (2015) Geochemical Characteristics of the Qahr-Abad Fluorite Deposit, Southeast of Saqqez, Western Iran. Arabian Journal of Geo-sciences.8:7309-7320.

10. Spoleto S, Stellato F, Marino A, Santoro L, (2016) Rare earth elements (REE)-Minerals in the Silius fluorite vein system (Sardinia, Italy). Ore Geology. Rev.74:211-224.

11. Rezaei A,Alipour S, Niroomand S,Samad A (2017) Rare earth element geochemistry and tetrad effects in fluorites: A case study from the Qahr-Abad deposit, Iran.N.Jb. Palont.Abh.283:255-273

12. Chakhmouradian A, Wall F (2012) Rare earth elements: minerals, mines, magnets (and more). Elements.8:333-342.

13. Hussein A, Aly M, El-Ramly M (1982) A proposed new classification of the granites of Egypt. J. Volcano. Geotherm. Res.14:187-198.

14. Yonan A (1990) Mineralogical, Petrochemical and Geochemical Studies on Granites Hosting Fluorite Mineralizations in the Eastern Desert of Egypt. Geologija.230

15. Fawzy K (1994) Geochemistry and Genesis of Fluorite Deposit, Homr Akarem,South Eastern Desert, Egypt. Moscow. Univ.122

16. Fawzy K (2001) Mineral composition and geochemistry of barite-fluorite mineralization at Wadi elsodmein, central eastern Desert, Egypt. Egypt. Mineral.13:27-43.

17. Fawzy K (2016) The Genesis of Fluorite Veins in Gabal El Atawi Granite, Central Eastern Desert, Egypt: Application of Fluid Inclusions Technique. Journal of African Earth Sciences, In Press.146:150-157

18. Fawzy K (2017) Characterization of a post orogenic a-type granite, gabal El Atawi, central eastern Desert, Egypt: geochemical and radioactive perspectives. Open J. Geol. 7:93-117.

19. Fawzy K, Solovova I, Babanskii A, Ryabchikov I (1996) Formation conditions of veined fluorite (Homrat Akarem, Egypt) inferred from an inclu-sion study. Geochem. Int. 14:32-35.

20. El-Mansi M (2000) Coloration of fluorite and its relation to radioactivity. Egypt. Min.12:93-106.

21. Surour A (2001) Fluid inclusions, distribution of REE and genesis of Abu Gerida fluorite mineralization, Central Eastern Desert, Egypt. The 5th Inter. Conf. on Geochemistry, Alex Univ., Egypt.7:353-371.

22. Salem I, Abdelmonem A, El-Shazly A, El-Shibiny N (2001) Mineralogy and geochemistry of Gabal El-Ineigi Granite and associated fluorite veins, Central Eastern Desert, Egypt: application of fluid inclusions to fluorite genesis. J. Afr. Earth Sci.32:29-45

23. Fawzy K, Abdel E (2002) Source and evolution of fluids of homretmukbid fluorite, SouthEastern Desert, Egypt. In: 6th Inter. Conf. On Geology of the Arab World. Cairo Univ.21:199-212.

24. Mohamed F, El-Sayed M (2008) Post-orogenic and anorogenic A-type fluorite-bearing granitoids, Eastern Desert, Egypt: Petrogenetic and geotectonic implications. Chemie der Erde.68:431-450.

25. Omar SAM (2010) Role of meteoric water in the genesis of fluorite mineralizationhosted by sheared granites at El-Missikat and El-Aradiya, central Eastern Desertof Egypt: evidence from fluid inclusions and wall rock alterations. January 2010. In: Fifth International Conference on the Geology of the Tethys Realm. SouthValley University.1-16.

26. Mohamed M (2013) Evolution of mineralizing fluids of cassiteritee, wolframiteand fluorite deposits from Mueilha tin mine area, Eastern Desert of Egypt, ev- idence from fluid inclusion. Arab. J. Geosci.6:775-782.

27. Mahdy N, Shalaby M, Helmy H, Osman A (2014) Trace and REE Element Geochemistry of Fluorite and Its Relation to Uranium Mineralizations, Gabal Gattar Area, Northern Eastern Desert, Egypt. Arabian Journal of Geosciences, 7:2573-2589   .

28. El Hadek H, Mohamed A, Bishara W, El Habaak G, Ali K (2016) Evolution of mineralizing fluids of greisen and fluorite veins, evidence from fluidinclusions. Int. J. Geophys. Geochem.3:49-56.

29. Sami M, Ntaflos T, Farahat E, Mohamed H, Hauzenberger C (2017) Mineralogical, geochemical and Sr-Nd isotopes characteristics of fluorite-bearing granites in the Northern ArabianNubian Shield, Egypt: Constraints on petrogenesis and evolution of their associated rare metal mineralization.Ore Geology Reviews.88:1-22.

30. Lindh A, Abu El-Rus MA, Mohamed MA, Olof Persson P, Scherstén A (2019) A model for granite evolution based on non-equilibrium magma separation: evidence from the Gharib and Qattar fluorite-bearing granites, Eastern Desert, Egypt. Article in International Journal of Earth Sciences.

31. Abu Dief A (1985) Geology of uranium mineralization in E1-Missikat, Qena-Safaga road, Eastern Desert, Egypt. M.Sc. Thesis. Faculty of Science, Al-Azhar University, Cairo.103

32. Ahmed N (1991) Comparative Studies of the Accessory Heavy Minerals in Some Radioactive Rocks of G. El-Misskat and G. El-Erediya, Eastern Desert, Egypt and their Alluvial Deposits, M.Sc. Thesis, Cairo Univ.244

33. Ibrahim T (2002) Geologic and radioactive studies of the basement-sedimentary contact in the area West Gabal El Missikat, Eastern Desert. Egypt. Ph. D Thesis. Faculty of science, Mansoura University.215.

34. Saleh G, Dawood Y, Abd El-Naby H (2002) Petrological and geochemical constraints on the origin of the granitoid suite of the Homret Mikpid area, south Eastern Desert, Egypt. Journal of Mineralogical and Petrological Sciences.97:47-58.

35. Saleh G, El Nisr S (2013) Tow Mica Granites, Southeastern Desert, Egypt: Geochemistry and Spectrometric Prospecting. Greener Journal of Geology and Earth Sciences.1:23-42.

36. Zoheir B, Emamb A (2012) Integrating geologic and satellite imagery data for high-resolution mapping and gold exploration targets in the South Eastern Desert. Egypt J Afr Earth Sci 66:22-34.

37. Boynton W (1984) Geochemistry of the rare earth elements: meteorite studies.In: Henderson, P. (Ed.), REE Geochemistry.63-114.

38. Moller P, Parekh P, Schneider H (1976) The application of Tb/Ca–Tb/La abundance ratios to problems of flourspar genesis. Mineralium Deposita 11:111-116.

39. Hill G, Campbell A, Kyle P (2000) Geochemistry of southwestern New Mexico fluorite occurrences: implications for precious metals exploration in fluorite-bearing systems. J. Geochem. Expl.68:1-20.

40. Sasmaz A, Yavuz F, Sagiroglu A, Akgul B (2005a) Geochemical patterns of the Akdagmadeni (Yozgat, Central Turkey) fluorite deposits and implications. J. Asian Earth Sci.24:469-479.

41. Sasmaz A, Onal A, Sagiroglu A, Onal M, Akgul B (2005b) Origin and nature of the mineralizing fluids of thrust zone fluorites in Çelikhan (Adiyaman, Eastern Turkey): a geochemical approach. Geochem. J.39:131-139.

42. Sasmaz A, Yavuz F (2007) REE geochemistry and fluid-inclusion studies of fluorite deposits from the Yaylagozü area (Yildizeli-Sivas) in Central Turkey. Neues Jahrb. Für Mineral.183:215- 226

43. Clark S, Petrman Z, Heier K (1966) Abundance of Uranium, Thorium and Potassium, In: Clark, S.P., Ed., Handbook of Physical Constraints, Geol. Soc. Am. Mem. 97, Geological Society of America, New York.521-541.

44. Worral F, Pearson D (2001) Water-rock interaction in an acidic mine discharge as indicated by rare earth element patterns. Geochem. Cosmochim. Acta 65:3027-3040.

45. Deng X, Chen Y, Yao J, Bagas L, Tang H (2014) Fluorite REE-Y (REY) geochemistry of the ca. 850 Ma Tumen molybdenite-fluorite deposit, eastern Qinling,China: constraints on ore genesis. Ore Geol. Rev.63,532-543.

46. Bau M, Dulski P (1995) Comparative study of yttrium and rare-earth element behaviors in fluorine-rich hydrothermal fluids. Contributions to Mineralogy and Petrology.119:213-223.

47. Irber W (1999) The lanthanide tetrad effect and its correlation with K/Rb, Eu/Eu*, Sr/Eu, Y/Ho, and Zr/Hf of evolving peraluminous granite suites. Geochim. Cosmochim.Acta.63:489-508.

48. Moller P, Morteani G (1983) On the chemical fractionation of REE during theformation of Ca-minerals and its application to problems of the genesis of oredeposits. In: Augustithis, S. (Ed.), The Significance of Trace Elements in Solving Petro-genetic Problems: Athens.747-791.

49. Constantopoulos J (1988) Fluid inclusion and REE geochemistry of fluorite from south-central Idaho. Econ. Geol. 83:626-636.

50. Eppinger G, Closs L (1990) Variation of trace elements and rare earth elements in fluorite: a possible tool for exploration. Econ. Geol. 85:1896-1907.

51. Palmer D, Williams A (1996) Genesis of the carbonatite hosted fluorite deposit at Amba Dongar, India: Evidence from fluid inclusions, stable isotopes and whole rock-mineral geochemistry. Econ. Geol.91:934-950.

52. Williams-Jones A, Samson M, Olivo R (2000) The genesis of hydrothermal fluorite-REE deposits in the Gallinas Mountains, New Mexico. Econ. Geol. 95:327-342.

53. Schwinn G, Markl G (2005) REE systematics in hydrothermal fluorite. Chem. Geol.216:225-248.

54. Möller P, Holzbercher E (1998) Eu anomalies in hydrothermal fluids and minerals. A combined thermochemical and dynamic phenomenon. Freib Forsch hefte.475:73-84. 55.

55. Bau M, Dulski P (1996) Distribution of yttrium and rare-earth elements in the Pengeand Kuruman iron-formations, Transvaal Supergroup, South Africa. Precambrian Res.79:37-55.

56. Schönenberger J, Köhler J, Markl G (2008) REE systematics of fluorides, calcite and siderite in peralkaline plutonic rocks from the Gardar Province, South Greenland.Chem. Geol. 247:16-35.

57. Heikal S, Khedr Z, Monsef M, Gomaa R (2019) Petrogenesis and geodynamic evolution of neoproterozoic Abu dabbab albite granite, central Eastern Desert of Egypt: petrological and geochemical constraints. J. Afr. Earth Sci.158:103518

58. Cambon A (1994) Uranium Deposits in Granitic Rocks. Notes on the National Training Course on Uranium Geologyand Exploration, Organized by IAEA and NMA, Cairo. Central Idaho. Econ. Geol.83:626-636.

Author Affiliation **Top**

Department of Economic Geology, Research Sector of Geology Nuclear, Materials Authority, Cairo, Egypt.